17th World Conference on Earthquake Engineering, 17WCEE
Sendai, Japan - September 13th to 18th 2020

SEISMIC-INDUCED DISPLACEMENT AND DISPLACEMENT CONTROL INDEX OF MASONRY CONCRETE REINFORCED SOIL RETAINING WALLS

CAI Xiaoguang(1), LI Sihan(2), HUANG Xin(3), XU Honglu(4), LIU Weiwei(5)

(1) *Director of Scientific Research Department(Office of International Affairs), Institute of Disaster Prevention, caixiaoguang123@163.com*
(2) *student, Institute of Engineering Mechanics China Earthquake Administration, lisihan@st.cidp.edu.cn*
(3) *student, Institute of Engineering Mechanics China Earthquake Administration, 154273083@qq.com*
(4) *student, Institute of Disaster Prevention, xuhonglu@163.com*
(5) *student, Institute of Disaster Prevention, 1539423927@qq.com*

Abstract

Excessive displacement is one of the main reasons for the loss of the structural function of the reinforced soil retaining wall(RSRW). Displacement failure modes of masonry concrete RSRW under earthquake loading are analyzed based on two large-scale shaking table tests. The geometric similarity ratios of two-tiered RSRW and single-tiered RSRW were deduced by dimensional analysis theories. The backfill was standard sand, the facing were masonry concrete and the reinforcements were geogrid. By testing the displacement response, the distribution law of horizontal displacement and residual displacement of the retaining wall are obtained. The test results show that, the middle section of the walls is outward bulge. With the increase of input acceleration, the horizontal displacement of the top model block increases until fall down. The maximum values of the horizontal displacement and residual displacement of the single/two-stage RSRW occur at the top of retaining wall. The overall displacement trend is an outwardly inclined arc. Based on the shaking table test results, displacement control indexes and the existing seismic damage evaluation criteria of the RSRW, the horizontal displacement control index in the seismic design of concrete block RSRW are proposed. The engineering damage assessment criteria are divided into four levels: basically intact, minor damage, medium damage, and damage. The research results can provide a reference for the seismic design of the concrete block RSRW and the rapid evaluation after the earthquake.

Keywords: masonry concrete reinforced soil retaining wall; shaking table test; horizontal displacement control index

1. Introduction

As a kind of flexible structure, reinforced soil retaining walls (RSRWs) have been used widely because of their many advantages, such as being simple structures, with strong adaptability. The RSRW mainly relies on deformation to absorb energy and reduce the impact of load on structures (Zhu et al. 2012[1]). Chen et al. (2007)[2] analysed its stress mechanism, in which the reinforcement and the soil are in a state of coordination deformation. The frictional dilatancy between the reinforcement and soil can function only when there is a relative displacement between them. The RSRW will have a large deformation; hence, to avoid affecting the use of the structure, it is necessary to control the deformation strictly. Therefore, lateral displacement control based on deformation is an important part of the design method of retaining walls, as has been reflected in the relevant specifications of many countries (Li 2007[3]; Wen et al. 2011[4]; Zhu et al. 2012[5]).

In particular, the lateral displacement control of the RSRWs, has been defined in relevant standards and specifications in many countries and regions (Yang et al. 2016[6]), as shown in Table 1. However, the most relevant standards or specifications above do not consider the effects of seismic motion. The authors consulted a large amount of literature and found that the seismic design of the displacement control of the flexible retaining wall has only sporadic regulations, such as *The New Zealand Bridge Handbook*.

Due to the wide application of the RSRWs, seismic design based on displacement control will be the most important part of geotechnical engineering. Two effective ways to study the displacement control of the RSRWs under earthquake action are earthquake damage investigations and shaking table testing. Earthquake damage investigation (Huang 2000[9]; Ling et al. 2001[10]; Zhuang et al. 2013[11]) is a direct method, and is reliable way of understanding the seismic mechanism, dynamic performance, and displacement control of the RSRWs. It is also an important basis for verifying existing theories, standards, test methods, and test results. Zhang et al. (2009)[12] proposed a three-stage seismic fortification theory considering 1% H, 3.5% H, and 6% H displacement of the retaining structure wall by investigating the retaining structure of the Sichuan disaster area. Zhu et al. (2012)[5] carried out statistics on the 49 retaining walls with large deformation, but no overall collapse, in the Wenchuan earthquake area. Considering the strong adaptability of the RSRW, the deformation control index should be within 4% H. The shaking table test consists of putting the model structure on the shaking table, and inputting the dynamic waves of time compression and amplitude change through the similarity ratio, which makes the structure bear lateral and vertical loads. Thus, the model and the prototype structures produce the same strain and damage form. The dynamic characteristics of the RSRW under different factors are studied by controlling the relevant conditions. Owing to its repeatability and short test cycle, the shaking table test was used by many scholars (Ling et al. 2005[13]; Huang et al. 2009[14]; Sander 2014[15]; Cai et al. 2018[16]). Cai et al. (1996)[17] studied the lateral displacement of the concrete block RSRW by shaking table test and actual engineering observation. And determined that the lateral displacement should be controlled within 1.5% H.

Table 1. Guidelines on horizontal displacement control

Standards or Specifications	Wall type	Maximum horizontal displacements	
		Value (mm)	x/H
WSDOT (2005)	Concrete panel	/	0.4% in 3m
	Welded wire	/	1.3% in 3m
	Wrapped face-permanent	/	1.7% in 3m
	Wrapped face-temporary	/	2.5% in 3m
FHWA (2008), AASHTO (2009)	all	/	0.9%–4%
NCMA (2009)	Modular-block	/	3.50%
PWRC (2005)	all	300	3%
EN 14475 (2006)	Modular-block	50	/
	Concrete panel	25	/
	Welded wire and gabion	100	/
BS8006 (2010)[7], Geoguide6 (2002)	all	/	0.50%
NGG (2005)[8]	all	/	0.1%–0.3%
New Zealand Bridge Handbook	all	150 (daily traffic >2500)	/
		200 (daily traffic <2500)	

RSRWs exhibit different performance under earthquake motion according to the varying wall types. Therefore, it is not appropriate to use the same lateral displacement control standard for RSRWs with different wall types. To address the inadequate research on lateral displacement control of modular-block RSRWs under seismic loading, the displacement mode of a modular-block RSRW was investigated by a large-scale shaking table test. Further, the lateral displacement control was analysed according to the test results, and an index of lateral displacement control suitable for modular-block RSRWs is proposed. We summarise the achievements and propose a displacement standard that can be used for rapid assessment after an earthquake. The results can provide theoretical support for the seismic design of modular-block RSRWs and the formulation of emergency rescue decisions.

2. Large-scale shaking table test

2.1 Test equipment

The experiments were performed on the Bidirectional Electrohydraulic Servo Seismic Simulation Shaking Table at the Civil Engineering Test Center of the Institute of Disaster Prevention. The main technical parameters of the shaking table were as follows: the table size was 3.0 m × 3.0 m; the bidirectional lateral seismic simulation was used; the maximum displacement was ± 100 mm in the X direction and ± 100 mm in the Y direction; the maximum acceleration was 2 g (full load) in the X direction and 2 g (full load) in the Y direction; and the maximum bearing was 20 t.

The acquisition system is mainly of two types: one is a domestic 128-channel dynamic acquisition system that can collected reinforcement strain data; the other is a domestic 16-channel acceleration acquisition system that can collect the table and soil acceleration data. The model box used for the test was fabricated using steel. The size of the model box: 3.0 m (length) × 2.0 m (height) × 1.5 m (width). The test model is presented in Figure 1.

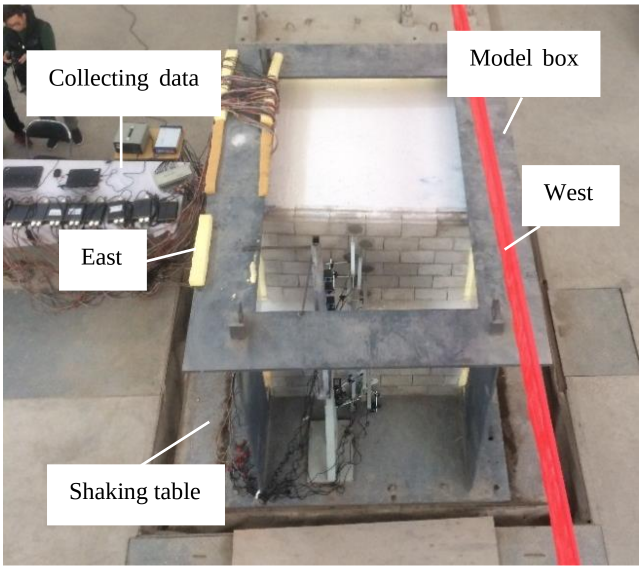

Figure 1. Model test equipment

2.2 Similitude rule

To reflect the engineering characteristics of the actual project as realistically as possible, and based on the bearing capacity of the shaking table and the size of the model box, the similarity ratio of two-step RSRW is 1:10. Furthermore, the similarity ratio of the single-step RSRW is 1:4 and 1:2. However, similarity designs (Iai 1989[18]; Zhang 1997[19]; Ling et al. 2005[20]; Cao et al. 2017[21]) generally cannot satisfy the similarity ratio for all parameters. Therefore, it is necessary to pay attention to the main factors affecting the test results, which neglecting the secondary factors.

2.3 Soil

The test uses standard soil as the backfill, the relative density of which is 70%. The physical and mechanical parameters are listed in Table 2. To strictly control the relative density strictly, the backfill is layered and filled, and the filling method is consistent with the method used by Wang et al. (2015)[22].

2.4 Wall

The model block size of the prototype project is 0.60 m (length) × 0.20 m (width) × 0.25 m (height), and is in accordance with the similarity ratio of 1:10. The model block size should be 0.060 m (length) × 0.020 m (width) × 0.025 m (height). To account for the small size of the blocks, and the model production, labour, and time costs, the two types of model blocks used in the test of Wang (2016)[23] were finally used: the size of model A was 0.25 m (length) × 0.15 m (width) × 0.15 m (height); the size of model B was 0.125 m (length) × 0.15 m (width) × 0.15 m (height).

Table 2. Physical and mechanical parameters of filling

Characteristic particle size (mm)			Non-uniform coefficient	Curvature coefficient	Maximum dry density (g/cm^3)	Internal friction angle (°)
d_{60}	d_{30}	d_{10}	C_u	C_c	ρ_d	φ
0.37	0.29	0.18	2.055	1.262	1.82	41

2.5 Geogrid

The geogrid has a low strength of the unidirectional geotechnical geogrid, EG50#. The length of the stretching unit, rib spacing, and rib thickness are 22.5, 2.22, and 0.1 cm, respectively. When the elongation of the unidirectional geotechnical geogrid is 2%, the tensile strength is 17.4kN/m. The arrangement of reinforcement is laterally isometric. With a vertical spacing of 15 cm. The lay length of the RSRW is 1.26 m. The model design of the RSRWs is shown in Figure 2.

2.6 Test setup

Figure 5 show the model of the RSRW, wherein the total height is 1.8 m. There are 16 displacement meters; among them, 12 displacement meters are placed at the centre of each panel to collect the seismic displacement data. Four displacement meters are placed at the top of the model, and their distances from the panel are 0.35, 0.70, 1.05, and 1.40 m. The vertical settlements of the model are collected under seismic response. The instrument layout used in the test is presented in Figure 3.

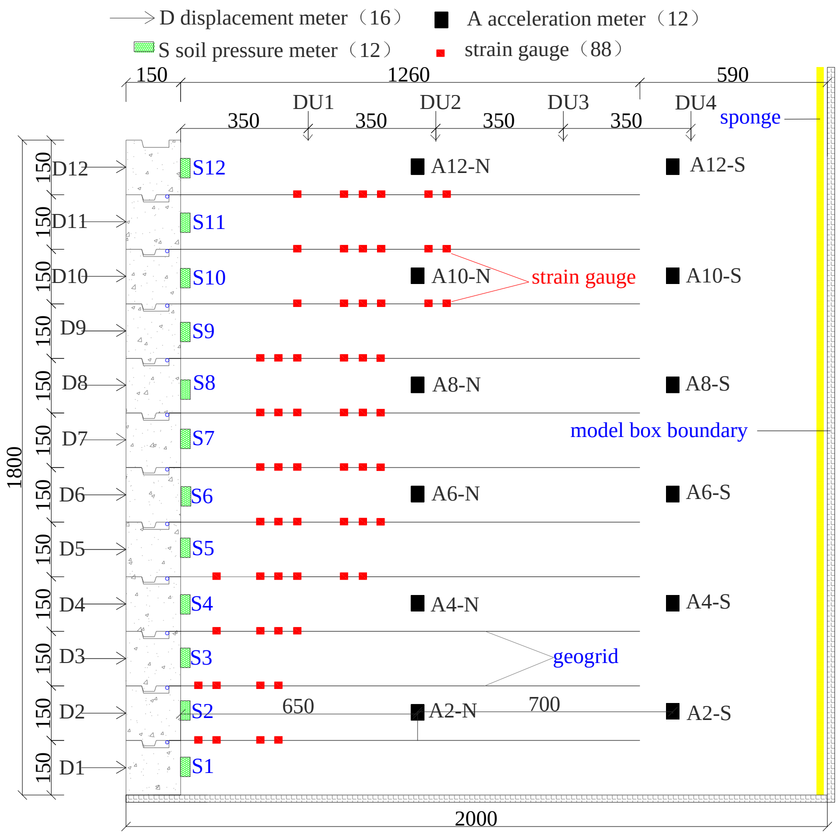

Figure 2. Shaking table test model of the RSRW

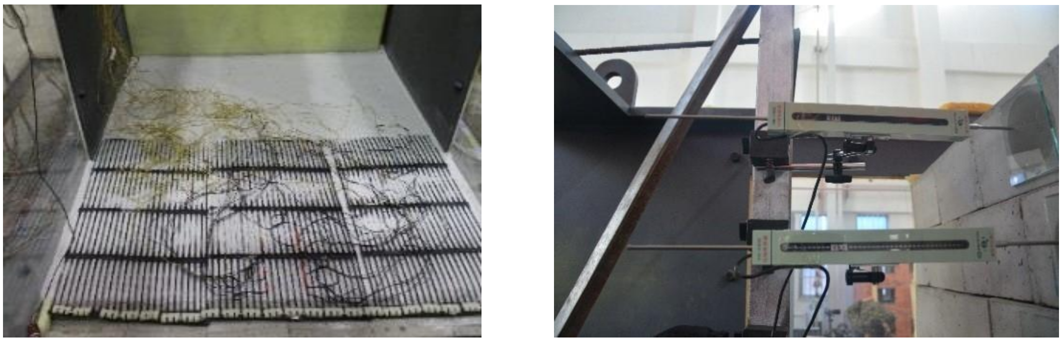

(a) (b)

Figure 3. Installation for test instruments: (a) laid geogrid; (b) ejector pins displacement meter

2.7 Test conditions

To understand the failure mechanism of the modular-block RSRWs, identify the failure phenomenon, and obtain the critical strains, the input acceleration is gradually increased until the retaining wall is damaged. The Wolong wave (WL) and El-Centro wave (EL) are input as a one-way lateral earthquake wave during the test. The peak acceleration of the WL is 1.0 g, and the time interval of the data points is 0.005 s. The peak acceleration of the EL is 1.0 g. and the time interval of the data points is 0.02 s. The duration is 58.5 s. The time and peak acceleration may be adjusted and compressed.

The tests are performed in increasing order of peak acceleration, and the time-compression ratio is from high to low. White noise is input before and after each change in wave magnitude. The loading cases are listed in Table 3.

Table 3. Loading cases RSRW

Case number	Input wave	PGA/g	Similarity ratio	Case code
	White Noise	0.05	1	WN
1, 2	WL, EL	0.1	4	WL0.1g, EL0.1g
3, 4	WL, EL	0.1	2	WL0.1g, EL0.1g
	White Noise	0.05	1	WN
5, 6	WL, EL	0.2	4	WL0.2g, EL0.2g
7, 8	WL, EL	0.2	2	WL0.2g, EL0.2g
	White Noise	0.05	1	WN
9,10	WL, EL	0.4	4	WL0.4g, EL0.4g
11,12	WL, EL	0.4	2	WL0.4g, EL0.4g
	White Noise	0.05	1	WN
13,14	WL, EL	0.6	4	WL0.6g, EL0.6g
15,16	WL, EL	0.6	2	WL0.6g, EL0.6g
	White Noise	0.05	1	WN
17,18	WL, EL	0.8	4	WL0.8g, EL0.8g
19,20	WL, EL	0.8	2	WL0.8g, EL0.8g
	White Noise	0.05	1	WN
21,22	WL, EL	1	4	WL1.0g, EL1.0g
23,24	WL, EL	1	2	WL1.0g, EL1.0g
	White Noise	0.05	1	WN
25,26	WL, EL	1.2	4	WL1.2g, EL1.2g
27,28	WL, EL	1.2	2	WL1.2g, EL1.2g

	White Noise	0.05	1	WN
29	WL	1.6	4	WL1.6g
30	WL	1.6	2	WL1.6g
	White Noise	0.05	1	WN
31	WL	2	4	WL2.0g
32	WL	2	2	WL2.0g

After each loading case, the data review, exterior damage recording, photographing, and other related work are performed. All the acquisition channels are then zeroed, and the model is treated as a new model for the next case until the model is destroyed.

3. Test results

3.1 Model damage phenomena

The damage of the RSRW is shown in Figure 4. The retaining wall under the earthquake motion first bulged in the middle and the surface mortar fell. Then, the lateral displacement of the top model block at the thirty-second case is so large that the whole top blocks of the model fall down and the model is destroyed.

The overall seismic response of the wall of the RSRWs is translation and rotation, and the partial blocks of each layer are relatively dislocated, as shown in Figure 5. Eventually, the model was damaged due to excessive displacement, and the results were consistent with those of Cai (1996)[17]. It can be seen that the horizontal displacement control of modular-block RSRWs is important.

(a) (b) (c) (d)

Figure 4. Seismic damage of the RSRW: (a) wall bulging; (b) sand drift; (c) block fall down; (d) wall failure

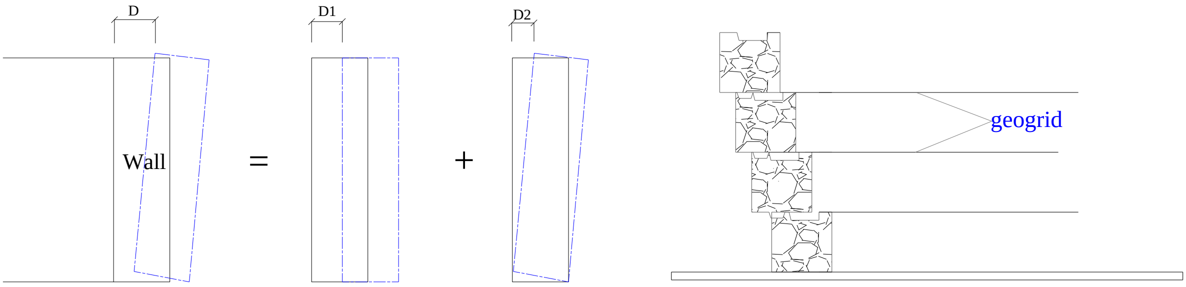

(a) (b)

Figure 5. Displacement observation: (a) overall displacement pattern; (b) inter-layer shift

3.2 Dynamic displacement

Figure 6 presents the displacement time history at D12 of the RSRW under cases 25 and 26. Due to the model block at the top of the retaining wall falls and hits some displacement meters under case 32, so all lateral displacement data under case 32 are not recorded.

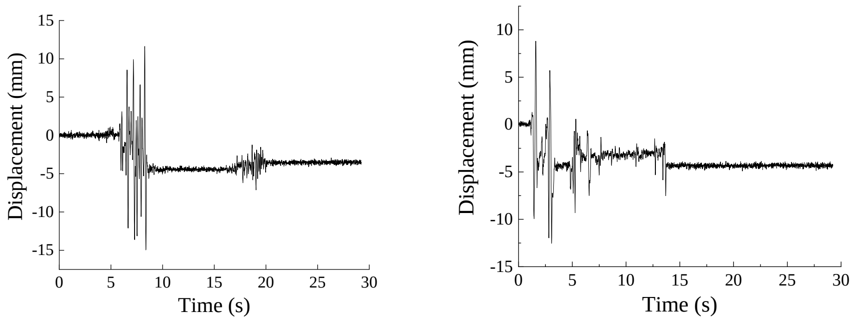

(a) (b)

Figure 6. Time history of lateral displacement at D12: (a) case 25; (b) case 26

To understand the overall displacement mode of the RSRW, take the maximum horizontal displacement acquired by D1–D12, and obtain the distribution of the horizontal displacement of the retaining wall along the height, as shown in Figures 7 and 8. It can be seen from the two figures that the increase in the horizontal displacement of the retaining wall from bottom to top gradually increases, as the peak acceleration increases, and the maximum displacement appears at the top.

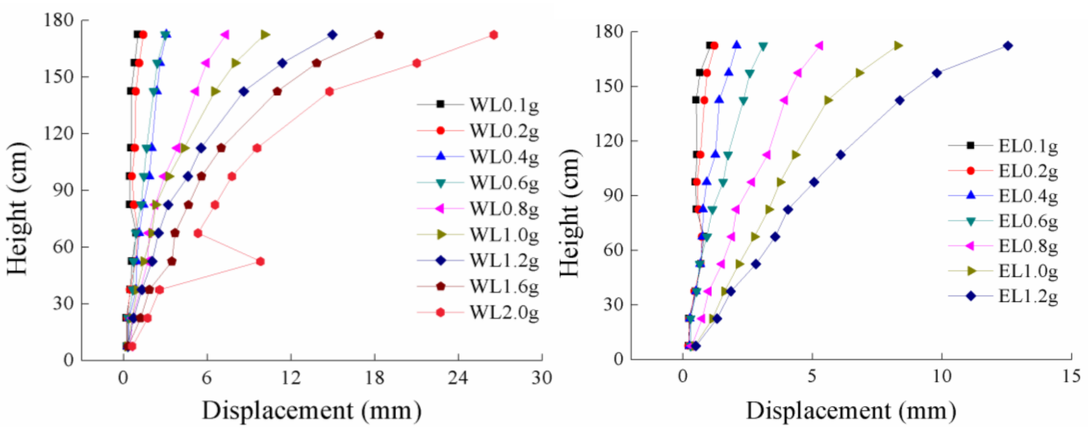

(a) (b)

Figure 7. Lateral displacement distribution along height (similarity ratio is 1:4): (a) WL; (b) EL

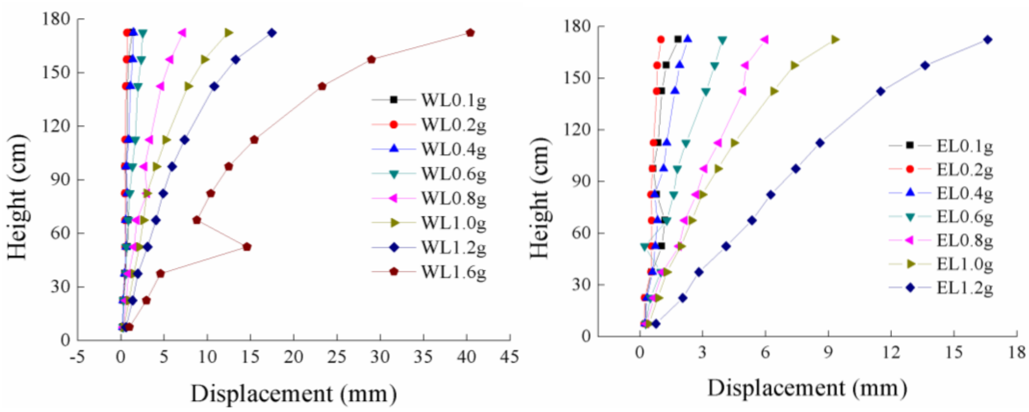

(a) (b)

Figure 8. Lateral displacement distribution along height (similarity ratio is 1:2): (a) WL; (b) EL

Figures 9 and 10 show the variation and rotation angle of the block displacement of each layer under different cases when the similar ratios are 1:4 and 1:2, respectively. It can be seen from the two graphs that the D/H ratio of each layer panel increases nonlinearly with the increase in PGA, and the top ratio is much larger than the bottom ratio; the D/H difference also increases with the increase in PGA. From this, it can be inferred the retaining wall not only produces translation under the action of the earthquake, but also rotates around the wall toe, showing a translational and rotational deformation mode. The angle of the retaining wall is proportional to the PGA, and the growth trend is consistent with the horizontal displacement trend of each layer of the retaining wall. Before the failure of the model, the D/H is 2.2% and the rotation angle is 1.4° during the vibration of case 30. During the vibration of case 31, the D/H reaches 1.5% and the rotation angle is 0.9°. Under the same seismic wave, the rotation angle and D/H size are different, indicating that the rotation angle and D/H are greatly affected by the input ground motion.

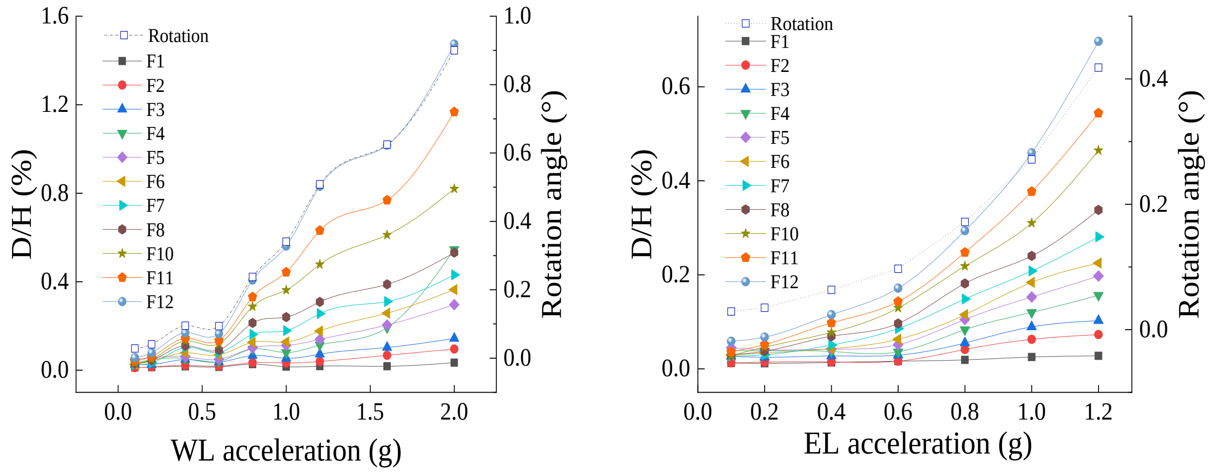

(a) (b)

Figure 9. Wall height ratio and wall rotation angle (similarity ratio is 1:4): (a) WL; (b) EL

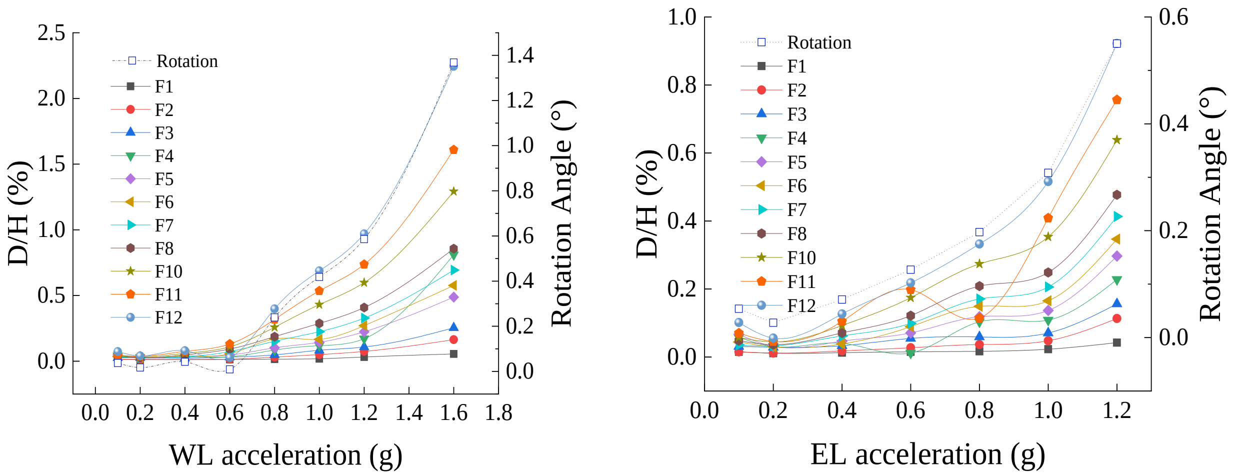

(a) (b)

Figure 10. Wall height ratio and wall rotation angle (similarity ratio is 1:2): (a) WL; (b) EL

3.3 Lateral displacement control index

It can be seen from Figures 6 that the retaining wall cannot be completely returned to the original position after the end of the dynamic action, as there is some residual displacement. The model after the end of each loading case is treated as a new model. The residual displacement of the RSRW can be seen in Figure 15 and 16.

It can be seen from Figures 11, and 12 that the retaining wall generally moves away from the backfilling direction, and the residual displacement is proportional to the PGA. When the PGA is less than 0.4 g, the residual displacement of each layer of model blocks is not much different, and a vertical line is approximated along the wall height. When the PGA is greater than 0.4 g, the residual displacement of each layer increases along the position of the measuring point, and the overall trend of the residual displacement is approximately an arc that is inclined to the outside of the wall. There is no sudden increase in residual displacement at each position, and the maximum residual displacement appears at the top. The residual displacement trend is consistent with the displacement trend during vibration, indicating that the geogrid plays a role in restraining the soil.

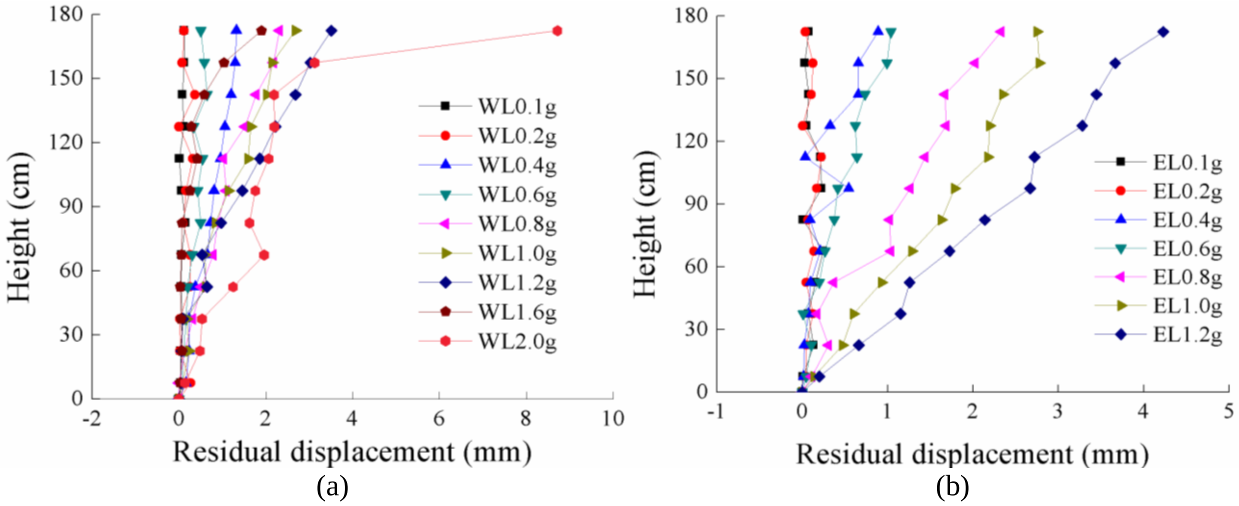

Figure 11. Residual displacement distribution of the RSRW (similarity ratio is 1:4): (a) WL; (b) EL

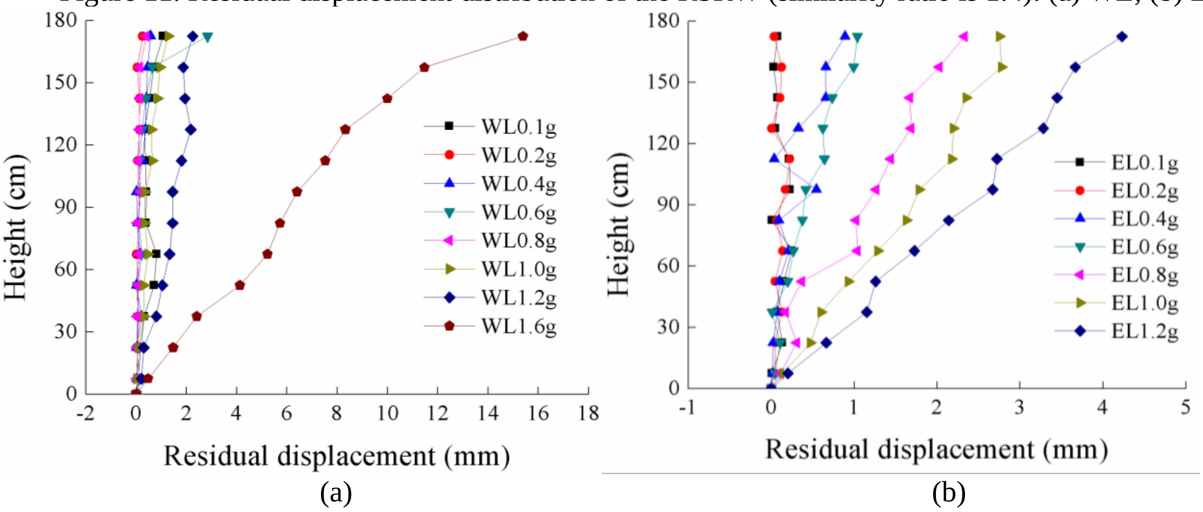

Figure 12. Residual displacement distribution of the RSRW (similarity ratio is 1:2) : (a) WL; (b) EL

The RSRW model was destroyed in case 9 before which no damage was observed. When the model is completed, it is regarded as model 1, and the model is regarded as model 2 after the end of case 8. At the time, the total residual displacement before the model is destroyed is the sum of all residual displacements of each loading case. A schematic diagram is shown in Figure 13.

Figure 14 shows the total residual displacement of RSRW before failure, and displacement control according to 1.5% (Cai et al. 1996), 3.5% H (Zhang et al. 2009), and 4% H (Zhu et al. 2012). It can be seen from figure that the maximum allowable lateral displacement of the RSRW is larger than 3.8% H. The maximum allowable lateral displacement is greater than 1.5% H according to Cai, or 3.5% H according to Zhang based on gravity retaining wall data, and less than 4% H according to Zhu. The maximum allowable lateral displacement of RSRW is considered. It is recommended to use 3.8% H as the lateral displacement control index in the seismic design of modular-block RSRW.

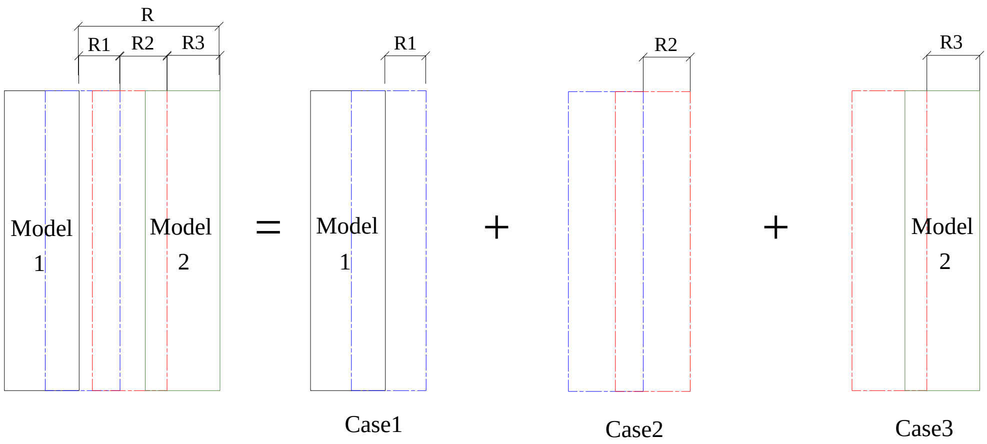

Figure 13. Schematic diagram of total residual displacement

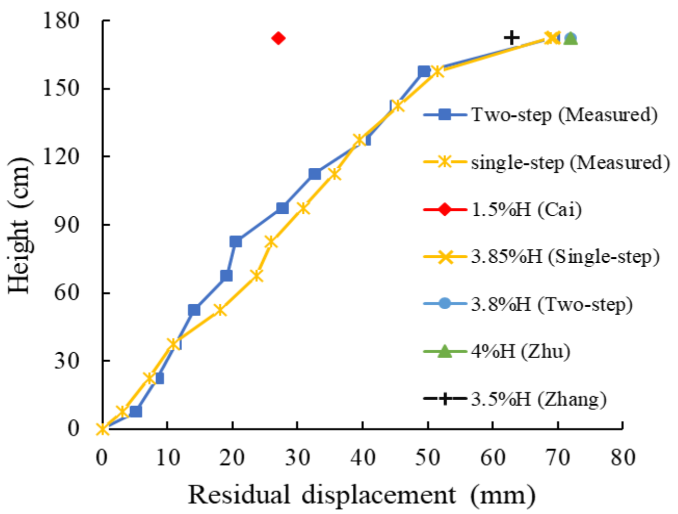

Figure 14. Total residual displacement distribution along wall height

4. Conclusions

Large-scale shaking table tests were performed to understand the seismic damage and lateral displacement mode of modular-block RSRWs. The lateral displacement control index of the seismic design of modular-block RSRW is obtained, and the seismic damage criterion of modular-block RSRWs are analysed. The following conclusions can be drawn:

(1) With regard to the middle section of retaining wall under the action of earthquake bulge, the greater the PGA, the greater the bulge. The lateral displacement of the top block increases with increasing PGA. Subsequently, the lateral displacement of top model is so large that the top model blocks fall down, and the retaining walls are destroyed.

(2) The lateral displacement increases with the increasing PGA. The lateral displacement at the top of the retaining wall reaches the maximum. RSRW are in translation mode of translation and rotation. When the similar ratio is different, the D/H ratio and rotation corner of the RSRW are greatly affected by the ground motion.

(3) The lateral residual displacement increases with the increasing PGA. The lateral residual displacement at the top of the retaining wall reaches the maximum. Considering the maximum allowable lateral displacement value in the results of modular-block RSRW and considering various displacement control indexes, the suggestion of lateral displacement control index of 3.8% H in seismic design of modular-block RSRW is proposed.

5. Acknowledgements

The authors appreciate the support of the National Natural Science Foundation of China (No.51778144) and Earthquake Technology Spark Program of China (XH204402).

6. References

[1] Zhu, H， W., Yao, L. K., Liu, Z. S.,& Chen, X. L. (2012). Research on seismic deformation characteristics of flexible wall. *Chinese Journal of Rock Mechanics and Engineering*, ,31（Supp.1）, 2829-2838. (in Chinese)

[2] Chen, X. L., Zhang, Y. L., Chen, X. M., & Zhou, X. Y., & Tao, X. X. (2007). Analysis of three aseismic questions and review on seismic response for new type of retaining walls, *WORLD EARTHQUAKE ENGINEERING*, 23(2): 118-124. (in Chinese)

[3] Li, Z. Q. (2007). Study on the aseismic dynamic reliability analysis and design based on the displacement method for the gravity type earth-retaining wall. Doctor thesis. Beijing Jiaotong University, Beijing, China. (in Chinese)

[4] Wen, C. P., Yang, G. L. (2011). Large-scale shaking table Tests study of seismic displacement mode of retaining structures under earthquake loading. *Chinese Journal of Rock Mechanics and Engineering*, 30(7): 1502-1512. (in Chinese)

[5] Zhu, H. W., Yao, L. K., Zhang, X. H. (2012). Comparison of dynamic characteristics between netted and packaged reinforced soil retaining walls and recommendations for seismic design. *Chinese Journal of Geotechnical Engineering*, 34(11): 2072-2080.(in Chinese)

[6] Yang, G. Q.， Xu, C.， Zhang, M. X et al. (2016) Geosynthetics Reinforcement Soil Structure Application Guidance. China Communications Press Co.,Ltd., Beijing, China,119-120 p. (in Chinese)

[7] BSI Standards Publication (2010). Code of practice for strengthened/reinforced soils and other fills.BS 8006-1:2010.

[8] Nordic Geosynthetics Group (2005). Nordic guidelines for reinforced soils and fills[S]. NGG Revision B-Oktober 2005.

[9] Huang,C.C. (2000). Investigations into the damaged soil retaining structures during the Chi-Chi earthquake. *Journal of Chinese Institute of Engineers*, 23(4): 417-428.

[10] Hoe, I. Ling., Dov, Leshchinsky., & Chou, N. N. S. (2001). Post-earthquake investigation on several geosynthetic-reinforced soil retaining walls and slopes during 1999 Ji-Ji earthquake of Taiwan. Soil *Dyn. Earthquake Eng*., 21(4): 297-313.

[11] Zhuang, W. L.， Chen, L. S. et al. (2013) Analysis of highways’ damage in the wenchuan earthquake-geological disaster and subgrade. China Communications Press., Beijing, China. (in Chinese)

[12] Zhang, J. J., Feng, J., Xiao, S. G.,& Liu, C. Q. (2009). Discussions on two key technical problems for seismic design of retaining structures. *Journal of Southwest Jiaotong University*, 44（3）：321-326. (in Chinese)

[13] Hoe, I. Ling., Yoshiyuki, Mohri., Dov, Leshchinsky., & Christopher, Burke.,& Kenichi, Matsushima., & Huabei Liu. (2005). Large-scale shaking table tests on modular-block reinforced soil retaining walls. *Journal of Geotechnical and Geoenvironmental Engineering*, 131(4): 465-476.

[14] Huang, C. C., Wu, S. H., Wu, H. J. (2009). Seismic displacement criterion for soil retaining walls based on soil strength mobilization. *Journal of Geotechnical and Geoenvironmental Engineering*, 135(1): 74-83.

[15] Andrew C. Sander, Patrick J. Fox, (2014). Ahmed Elgamal. Full-scale seismic test of MSE retaining wall at UCSD [C]. *Geo-Congress* 2014.

[16] Cai, X. G., Li, S. H., Huang, X. (2018). Shaking table tests on dynamic characteristics of two-stage reinforced soil-retaining wall. *China J. Highw Transp*, 31(2): 200-207.

[17] Z. Cai., R. J. Bathurst. (1996). Seismic-induced permanent displacement of geosynthetic-reinforced segmental retaining walls. *Can. Geotech. J.*, 33: 937-955.

[18] Susumu Iai. (1989). Similitude for shaking table tests on Soil-Structure-Fluid model in 1g gravitational field, *Soils and Foundations*, 29(1): 105-118.

[19] Zhang, M. Z. (1997). Study on similitude laws for shakingtable tests. *Earthquake Engineering and Engineering Vibration*, 17(2): 52-58. (in Chinese)

[20] Ling, X. Z., Wang, C., Wang, C. (2005). Scale modeling method of shaking table test of dynamic interaction of pile-soil-bridge structure in ground of soil liquefaction. *Chinese Journal of Rock Mechanics and Engineering*, 24(14)：2428-2433. (in Chinese)

[21] Cao, L. C., Zhang, J. J., Fu, X., & Zeng, P. Y. (2017). Strain response of the stripe reinforced soil with rigid retaining wall. *Chinese Journal of Rock Mechanics and Engineering*, 36(7)：1768-1779. (in Chinese)

[22] Wang, L. Y., Chen, G. X., Chen, S. (2015). Experimental study on seismic response of geogrid reinforced rigid retaining walls with saturated backfill sand, *Geotextiles and Geomembranes*, 43: 35-45.

[23] Wang, H. (2016). Research on structural behavior of geogrid reinforced soil retaining wall under static or dynamic loads. Doctor thesis. Beijing Jiaotong University, Beijing, China. (in Chinese)

